Accepted Manuscript

Pt(IV) prodrugs containing microtubule inhibitors displayed potent antitumor activity and ability to overcome cisplatin resistance

Lingxue Li, Xiaochao Huang, Rizhen Huang, Shaohua Gou, Zhimei Wang, Hengshan Wang

PII: S0223-5234(18)30572-5

DOI: 10.1016/j.ejmech.2018.07.016

Reference: EJMECH 10551

To appear in: *European Journal of Medicinal Chemistry*

Received Date: 24 October 2017

Revised Date: 2 July 2018

Accepted Date: 6 July 2018

Please cite this article as: L. Li, X. Huang, R. Huang, S. Gou, Z. Wang, H. Wang, Pt(IV) prodrugs containing microtubule inhibitors displayed potent antitumor activity and ability to overcome cisplatin resistance, *European Journal of Medicinal Chemistry* (2018), doi: 10.1016/j.ejmech.2018.07.016.

Graphical abstract

Pt(IV) prodrugs containing microtubule inhibitors displayed potent antitumor activity and ability to overcome cisplatin resistance

Lingxue Li, [a 1] Xiaochao Huang, [a 1] Rizhen Huang, [a] Shaohua Gou, [a *] Zhimei Wang, [a] and Hengshan Wang [b *]

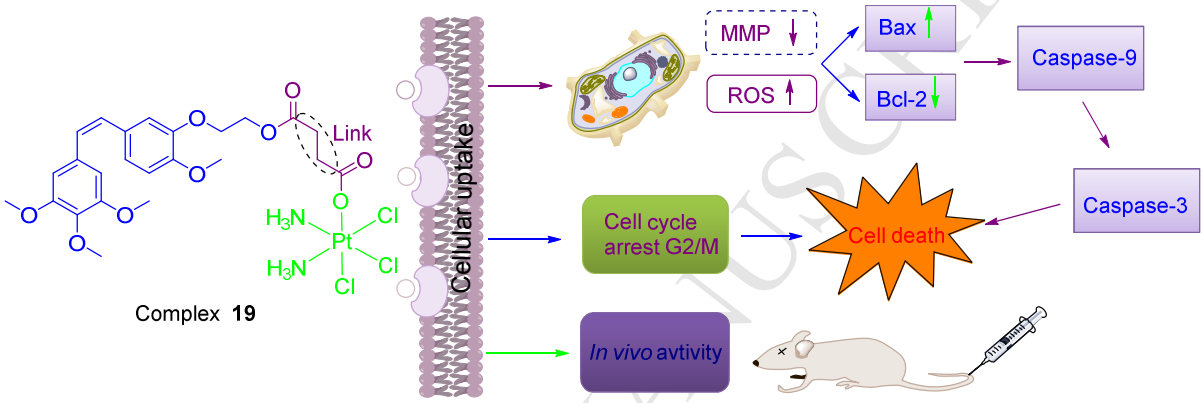

Pt(IV) prodrugs containing microtubule inhibitors displayed potent antitumor activity and ability to overcome cisplatin resistance

Lingxue Li, [a 1] Xiaochao Huang, [a 1] Rizhen Huang, [a] Shaohua Gou, [a *] Zhimei Wang, [a] and Hengshan Wang [b *]

[a] Jiangsu Province Hi-Tech Key Laboratory for Biomedical Research, Southeast University, Nanjing 211189, China.

[b] State Key Laboratory for the Chemistry and Molecular Engineering of Medicinal Resources, School of Chemistry and Pharmaceutical Sciences of Guangxi Normal University, Guilin 541004, China.

Abstract

It is well-known that cisplatin exhibited a broad spectrum of anticancer activities against many solid tumors, but its severe toxicity and drug resistance have largely limited wider clinical applications. Various strategies have been tried to discover new Pt(II) drugs with at least equal activity as well as low toxicity compared to cisplatin, but the inherent problem remains unsolved. Here we report that Pt(IV) complexes comprising a CA-4 analogue, as dual-targeting Pt(IV) prodrug, were synthesized and evaluated for anti-proliferative activity using MTT assay. Among them, complex **19** displayed most potent activity against the tested cancer cell lines, and simultaneously exhibited better cell selectivity between cancer cells and normal cells than that of cisplatin. Mechanism studies revealed that complex **19** effectively induced cell cycle arrest at the G2/M phase and dramatically disrupted the microtubule organization. Moreover, complex **19** significantly induced cell apoptosis and decreased MMP. Importantly, complex **19** significantly inhibited tumor growth in SK-OV-3 xenograft model *in vivo* without apparent toxicity.

Keywords: Pt(IV) complex; Antitumor activity; Tubulin; Apoptosis

* Corresponding author.

Corresponding author: E-mail addresses: sgou@seu.edu.cn (S. Gou), whengshan@163.com (H.-S. Wang).

[1] Co-first author: These authors contributed equally to this work.

1. Introduction

Ptlatinum(II)-based anticancer drugs, such as cisplatin (CDDP), carboplatin and oxaliplatin (OXP) are widely used for the treatment of many solid tumors as first-line chemotherapeutic agents in clinic. [1-5] Mechanism studies indicated that they induce apoptosis in cancer cells mainly through DNA damage. [6-8] However, non-specificity of these drugs toward cancer cells has limited their applications. [9-11] In the last two decades, various Pt(II) complexes have been synthesized and screened for antitumor activity, but, unfortunately, only a few of compounds entered clinical trials and most of them failed. [12] Trying to get rid of the embarrassment, researchers focused on inert Pt(IV) complexes as prodrugs that can be activated by intracellular reduction and reduced to Pt(II) equivalents following cellular uptake. [13, 14] For example, satraplatin, which used to be a promising Pt(IV) prodrug, entered phase III clinical trials for an orally active drug against prostate cancer due to better stability, lower toxicity, and higher blood circulation time than cisplatin. [15, 16] In addition, several research groups reported that Pt(IV) prodrugs containing biologically active units in the axial position could significantly improve the antitumor activities and overcome the side effect of Pt(II) drugs (**Fig.1**). [17-22]

The chemotherapeutic agent combretastatin A-4 (CA-4, **Fig. 2**), a naturally occurring *cis*-stilbene from the bark of the South African Cape Bushwillow (*Combretum caffrum*), was found to show potent antitumor activity against many types of human cancer cells, own capability to bind the colchicine binding site of tubulin, and interfere with the polymerization of tubulin. [23-25] Its derivatives, compounds **7** and **17**, also exhibited excellent anticancer activities against a number of human cancer cells including multidrug resistant cancer cell lines in addition to strongly inhibit tubulin polymerization via combining the colchicine binding site [26, 27]. Moreover, combretastatin A-4-phosphate (**1a**, **Fig. 2**) and serine amino acid analogue of CA-4 (AVE8062, **Fig. 2**) in combretastatin family are currently under clinical trials as a single drug or in combination for anticancer therapy. [28, 29] To overcome resistance of cisplatin and reduce its side effect, researchers now prefer to use combination chemotherapy treating the patients with other therapeutics drugs that act by different mechanisms. [13] Recent studies indicated that the combination of platinum anticancer agents with tubulin inhibitors, primarily with paclitaxel and docetaxel, could result in improved therapeutic profiles. [30] Schobert and co-workers recently reported Pt(II) complexes containing chalcone derivatives **2a** and **3a** (**Fig. 2**), which displayed

moderate antitumor activities against certain types of solid tumors mainly due to the DNA-damage Pt(II) agents and tubulin-targeting chalcone moieties. [31] Therefore, a combination of platinum anticancer agents with tubulin inhibitors can be an effective strategy to overcome drug resistance and enhance therapeutic effects.

Based on the above background, we have designed a new series of dual-targeting Pt(IV) prodrugs, which are expected not only to carry the DNA damaging platinum-based agent warhead into the tumor cells, but also have a CA-4 derivative **7** or **17** to inhibit tubulin polymerization. Herein, we report the synthesis and biological activities of these compounds as well as their underlying mechanism of actions.

2. Results and discussion

2.1. Design and synthesis

The synthetic route to prepare compounds **12-13** and **19-20** are depicted in Schemes **1** and **2**. Firstly, the CA-4 derivatives **7** and **17** were obtained according to the reported procedures. [26, 28] On one hand, compound **8** was achieved by the formation of amide bond between **7** and mono-methyl glutarate in the presence of HOBT/EDCI, which was followed by hydrolysis of **8** with aluminum hydroxide in the presence of THF/H_2O to obtain the acid **9**. On the other hand, compound **18** was achieved by treatment of compound **17** with succinic anhydride in the presence of Et_3N in DMF. Meanwhile, Pt(IV) complexes **10** and **11** were prepared through the oxidative chlorination of the corresponding Pt(II) complexes (cisplatin or oxaliplatin) with N-chlorosuccinimide (NCS) in water according to the former methods. [32] Finally, target compounds **12-13** and **19-20** were obtained by esterification between **9** or **18** and **10** or **11** in the presence of TBTU/Et_3N. The resulting target compounds were characterized by ^{1}H NMR and ^{13}C NMR spectra together with ESI-MS spectroscopy.

2.2. In vitro cytotoxicity.

The *in vitro* cytotoxicity of complexes **12-13** and **19-20** were evaluated by MTT assays on three human cancer cell lines, HCT-116 (colorectal), HepG-2 (hepatocellular), MGC-803 (gastric) and two normal cells NCM460 (colon) and HL-7702 (liver), using cisplatin, oxaliplatin, **7**, **17** and **CA-4** as the positive controls, respectively. The IC_{50} values (concentration required to reduce viability to 50%) were summarized in Table 1. *In vitro* evaluation results revealed that compounds **7** and CA-4 displayed excellent antitumor activities against the tested three human cancer cells as

expected, but CA-4 analogues **9** and **13** exhibited lower cytotoxicity than the positive drugs **7** and **17**. It was noted that complexes **12-13** and **19-20**, the Pt(IV) derivatives of cisplatin or oxaliplatin with one CA-4 analogous ligand in the axial position, possessed higher cytotoxicity against all test cancer cell lines than cisplatin and oxaliplatin. Especially, complexes **12** and **19** possessed better antitumor activities against all test cancer cell lines than cisplatin, with IC_{50} values in the range of 0.62–0.97 μmol/L (**12**) and 0.39–0.71 μmol/L (**19**), which showed 8.6~14.4 (**12**) and 11.8~21.8 (**19**) fold increase in activity than those of cisplatin. In addition, both **12** and **19** synchronously exhibited lower cytotoxicity toward two normal cells NCM460 and HL-7702 than cisplatin and CA-4, respectively. Moreover, Pt(IV) complexes **13** and **20** significantly exhibited better anti-proliferative activity against the tested cancer cell lines than oxaliplatin, with IC_{50} values in the range of 0.75–1.21 and 0.52–1.06 μmol/L, respectively. Interestingly, complex **19** showed significantly more effective anticancer activity than compound **17** against the tested three human cancer cells, and exhibited up to 1.7~2.6 fold increased cytotoxicity compared with compound **17**. More importantly, the selectivity index of complexes **12** and **19** were calculated out as 36.7, 20.9 and 43.6, 49.6, respectively, much higher than that of cisplatin (1.4 and 1.3). The similar results were also observed in complexes **13** and **20**. In short, the *in vitro* evaluation results suggested that these Pt(IV) complexes showed better cell selectivity between cancer cells and normal liver cells than those of cisplatin and oxaliplatin.

2.3. Antitumor activity of target complexes against cisplatin resistant cancer cell line.

Drug resistance is an important therapeutic problem that confined the efficacies of cisplatin for some human cancer cells. Thus, we further evaluated the cytotoxicity of complexes **12-13** and **19-20** against cisplatin sensitive and resistant cancer cells (human ovarian cancer cells SK-OV-3 and SK-OV-3/CDDP)). As shown in Table 2, the IC_{50} value of cisplatin against SK-OV-3/CDDP resistant cells was increased to 30.57 μmol/L. While in contrast, the corresponding IC_{50} values of complexes **12** and **19** against SK-OV-3/CDDP resistant cells did not obviously change compared with those against cisplatin sensitive cells. It was much significant to observe that complexes **12** and **19** had much lower resistance factors (1.25 and 1.26) compared with cisplatin (5.99). Interestingly, other Pt(IV) complexes **13** and **20** were also found to exhibit obvious anticancer activities against cisplatin resistant SK-OV-3/CDDP cells comparable to oxaliplatin with small resistance factors. The results indicated that these Pt(IV) complexes with almost equal potent

activity against cisplatin-resistant cells might be useful in the treatment of drug refractory cancer resistance to other platinum drugs.

*2.4 HPLC analysis of releasing ability of the typical target compound **19.***

In order to investigate whether compound **9** or **18** and divalent Pt(II) species can be released from target compounds (**12-13** or **19-20**) by biomolecular reducing agents such as ascorbic acid, we incubated a typical compound, **19**, in a solution of acetonitrile and water (13:7) in the presence of ascorbic acid (0.5 mmol/L) at 37 □, and analyzed the liberation of compound **19** and cisplatin over a period of 12 h by HPLC chromatograms. As shown in **Fig. S1**, compound **19** can be easily reduced to compound **18** and the corresponding Pt(II) equivalent under the test condition as time passed, accompanied by the falling down peak of compound **19** and the rising up peak of compound **18** in a time-dependent mode. Notably, cisplatin was not observed in the HPLC chromatograms due to its weak chromophore in the ultraviolet detecting condition. In short, these results suggested that the target compound can be easily reduced to release the corresponding Pt(II) equivalent and compound **9** or **18** under reduction, indicating their potential biological activity.

*2.5. Complex **19** induced apoptosis in SK-OV-3 cells.*

Studies suggested that most metal complex anticancer drugs generally kill cancer cells by activating apoptosis. [33] Because complex **19** was found to exhibit broad spectrum antitumor activity against all tested human cancer cells and the best activity against SK-OV-3 cancer cells *in vitro*, it was chosen to be further investigated on the mechanism of action. The apoptosis of SK-OV-3 cells induced by complex **19** was studied using FITC-Annexin V staining and propidium iodide (PI) staining method, in which Q1, Q2, Q3, and Q4 represent four different cell states: necrotic cells, late apoptotic or necrotic cells, apoptotic cells and living cells, respectively. The percentages of apoptotic cells were determined by flow cytometry. SK-OV-3 cells were treated with complex **19** and cispaltin at the indicated concentrations for 24 h, respectively. As shown in **Fig. 3**, SK-OV-3 cells treated with complex **19** exhibited a concentration-dependent increase of apoptosis by 29.4% and 44.5% at 5 and 10 μmol/L, respectively. In contrast, the percentage of apoptosis cells was 23.98% after incubation with cisplatin at 10 μmol/L for 24 h, which was obviously lower than that of complex **19** under the same condition. These results clearly revealed that complex **19** could effectively induce apoptosis in SK-OV-3 cancer cells at the indicated concentrations.

2.6. Hoechst 33258 staining.

The ability of complex **19** to induce apoptosis was further investigated by analyzing the nuclear morphology of the exposed SK-OV-3 using Hoechst 33258 staining. SK-OV-3 cells were treated with complex **19** and cisplatin at the indicated concentrations for 24 h, and then stained by Hoechst 33258 to detect apoptosis morphologically under the fluorescence microscope. As shown in **Fig. 4**, the control cells exhibited weak blue fluorescence and appeared as regular round contours. Following treatment with complex **19**, most cells emitted brilliant blue fluorescence, and the nuclei of SK-OV-3 cells appeared hyper condensed (brightly stained). The number of apoptotic nuclei containing condensed chromatin obviously increased when SK-OV-3 cells were treated with complex **19** (10 μmol/L) for 24 h (**Fig. 4**), suggesting that apoptosis of SK-OV-3 cells was significantly induced by complex **19** in a concentration-dependent manner, consistent with the results for FITC-Annexin V staining and propidium iodide staining.

2.7. Cellular uptake.

It is well known that the cytotoxicity of current Pt(II)-based anticancer agents, such as cisplatin and oxaliplatin, was associated with the uptake of platinum, hence the cellular uptake measurement of complex **19** was carried out. The platinum content in SK-OV-3 cells was analyzed using ICP-MS after 24 h of incubation with complex **19** and cisplatin. As shown in Table 3, the whole uptake of complex **19** in the SK-OV-3 cells was 335±31 (5 μmol/L) and 709±70 ng Pt per 10^6 cells (10 μmol/L), respectively, obviously higher than those of cisplatin under the same conditions. Interestingly, the cellular platinum of compound **19** was up to 2.2-fold increase at high dose in SK-OV-3 cells compared to cisplatin under the same concentration. In addition, it was notable that the data was completely in accordance with the MTT assay (IC_{50} value in SK-OV-3: **19** > cisplatin), which suggested that introduction of a CA-4 analogue in the axial position of the related Pt(IV) complex can effectively improve the cellular uptake and eventually result in the increase of its antitumor activity.

2.8. TUNEL staining.

Many studies indicated that the cytotoxicity of platinum-based drugs are able to induce DNA damage [34], thus, we further investigated the effect of complex **19** on the integrity of DNA in SK-OV-3 cells using TUNEL staining according to a method reported previously [35]. As shown in **Fig. 5**, the cells with increased green florescence intensity (in the web version) suggested the

degree of DNA damage induced by cisplatin at the indicated concentration as expected. Interestingly, complex **19**-treated SK-OV-3 cells significantly exhibited enhanced green florescence intensity (in the web version) in a concentration-dependent manner compared to the control cultures, suggesting the presence of terminal DNA damage caused by complex **19**.

2.9. Cell cycle analysis.

In order to further understand the effect of the synthetic Pt(IV) complex **19** on cell cycle arrest, we used flow cytometry to detect the cell cycle distribution of SK-OV-3 cells following a 24 h treatment with complex **19** at the indicated concentrations. Untreated cells were served as a negative control, and cells treated with cisplatin were acted as a positive control. As shown in **Fig. 6** A and B, complex **19** were found to be as effective in arresting the cell cycle at G2/M phase in a concentration-dependent manner compared with the control. With the untreated SK-OV-3 cells, the percentage of cells in the G0/G1 phase was at 75.37% with only 5.05% in the G2/M phase. After treatment with cisplatin at 10 μmol/L, the percentage of cells in the G2/M phase only increased to 11.88%, while in the cells treated with complex **19** at 5 and 10 μmol/L, the percentage of cells in the G2/M phase increased to 27.11% and 67.84%, respectively. These trends were in accordance with the current anti-mitotic agents, suggesting that tubulin might probably be an effective target for complex **19**.

*2.10. Complex **19** regulated the expression of G2/M-related proteins.*

In order to further investigate the molecular mechanism of complex **19** induced G2/M phase block, the expression of cell division regulated proteins (major Cdc2, cyclin B1, and Cdc25c) were confirmed by immunoblotting analyses. As shown in **Fig. 6** C and D, compared with the vehicle treated control, complex **19** caused a significant decrease in Cdc2, cyclin B1, and Cdc25C expression in a concentration-dependent manner. These results, which were consistent with the cell cycle analysis assay, further suggested the mechanism of the cell cycle arrest effect.

2.9. Analysis of immunofluorescence staining.

It is well-known that the biological activity of CA-4 and its analogues has been reported to be bound up with tubulin [24, 26]. In order to further evaluate whether the antitumor activity of complex **19** was derived from an interaction with tubulin, SK-OV-3 cells were treated with complex **19** and CA-4 at the indicated concentrations for 24 h to analyze the cellular microtubule network by immunohistochemistry followed by nuclear staining with 4,

6-diamidino-2-phenylindole (DAPI). As shown in **Fig. 7**, a well-organized microtubule network throughout the cells was observed in the control group, while cells treated with CA-4 exhibited severely disrupted microtubule organization compared with the control group as expected. Importantly, it was noted that cells treatment with complex **19** obviously disrupted microtubule organization compared with untreated cells. These results demonstrated that complex **19** dramatically disrupted the microtubule organization in a concentration-dependent manner, and further revealed that tubulin was an effective target for its anticancer activity.

*2.11. Complex **19** triggered mitochondrial pathway dependent apoptosis.*

Many recent researches demonstrated that mitochondria play an important role in the progression of apoptosis. [36, 37] The loss of mitochondrial membrane potential (MMP) has been implicated as an early event in apoptotic cells. In order to learn whether apoptosis induced by complex **19** was related to mitochondrial dysfunction, cells treated with complex **19** at the indicated concentrations for 24 h and the MMP were examined by fluorescence microscope using JC-1 and Hoechst 33258 staining. Untreated cells were used to serve as a negative control, and cells treated with cisplatin were used to act as a positive control. In the control group (untreated cells), JC-1 existed as aggregates in the mitochondria (red), while the apoptotic and necrotic cells, JC-1 existed as a monomer in the cytosol (green). As shown in **Fig. 8**, treatment of SK-OV-3 cells with complex **19** and cisplatin, respectively, caused a decreased MMP level at the indicated concentration for 24 h.

*2.12. Complex **19** triggered ROS generation.*

Because mitochondrial dysfunction is associated with mitochondrial production of reactive oxygen species (ROS),[38] we further evaluated whether ROS production increased after treatment with complex **19** at the indicated concentrations. The fluorescent probe 2, 7-dichlorofluorescein diacetate (DCF-DA) was used to detect by flow cytometry after cells treated with the test compounds for 24 h. Untreated cells served as a negative control, and cells treated with cisplatin acted as a positive control. As shown in **Fig. 9**, both complex **19** and cisplatin induced the production of significant amounts of ROS in comparison with control cells, in agreement with the dissipation of MMP. Interestingly, after exposure to 10 μmol/L of complex **19** for 24 h, the ROS level was 75.2%, which showed up to 3.3-fold increase in SK-OV-3 cells compared to cisplatin under the same concentration. Altogether, these results proved that complex

19 induced apoptosis through the mitochondrial pathway.

*2.13. Complex **19** induced apoptosis via the activation of caspases and regulated apoptosis-related protein expression.*

Caspases, in general, are a family of cysteine proteases that play an important role in apoptosis. [39] In order to investigate whether complex **19** induced caspase-dependent cell death, we performed an immunoblot analysis of the activation of two caspases, namely caspase-3 and -9, which are involved in the apoptotic mitochondrial pathway. As shown in **Fig.10** A and B, exposure of SK-OV-3 cells to complex **19** resulted in the activation of caspase-3 and caspase-9 in a concentration-dependent manner. In addition, many studies indicated that Bcl-2 family proteins are crucial components of mitochondrial stress-induced cellular apoptosis [40, 41], hence, the expression of apoptosis-related proteins (Bax, pro-apoptotic protein and Bcl-2, anti-apoptotic protein) was also investigated. Western blot analysis suggested that complex **19** significantly up-regulated the expression of Bax and correspondingly down-regulated the expression of Bcl-2.

2.14. Antitumor effect of complex **19** *in vivo.*

To evaluate the efficacy of complex **19** to inhibit tumor growth *in vivo*, we established the nude mouse SK-OV-3 tumor xenograft models by subcutaneously injecting SK-OV-3 cells in the logarithmic phase into the right armpit of the mice. When the model was well-established, mice with tumors at the volume of 100-150 mm^3 were randomly divided into six groups (n=5/group): (1) vehicle treated group (5% dextrose injection), (2) complex **19** (5 mg/kg) treated group, (3) complex **19** (13 mg/kg) treated group, (4) cisplatin (5 mg/kg) treated group; (5) CA-4 (5 mg/kg) treated group; (6) equal mass mixture of cisplatin (5 mg/kg) + CA-4 (5 mg/kg) treated group. As shown in **Fig. 11 A** and D, the growth of SK-OV-3 tumor xenograft was effectively suppressed by 53.1% and 60.5% (percentage of inhibition rate [IR] values) after treatment groups were injected with complex **19** at two doses (5 and 13 (mg/kg)/7 days) for 21 days in the SK-OV-3 tumor model. Interestingly, complex **19** exhibited better antitumor activity than CA-4 (IR, 51.6%) *in vivo* in the entire observation period, as shown in **Fig. 11** B. It was noticed that complex **19** exhibited better antitumor activity *in vitro*, while displayed a little lower value of IR *in vivo* than that of cisplatin (IR, 65.8%) and the combination of cisplatin+CA-4 (IR, 69.7%), respectively. Although the cisplatin effectively caused tumor growth inhibition, its toxicity was conspicuously obvious, as evidenced by loss of body weight compared with complex **19** in the entire observation period (**Fig.**

11 C). Notably, it was found that conjugation of cisplatin with CA-4 not only improved therapeutic effects, but also reduced the toxicity of cisplatin as evidenced by the inhibition of tumor growth and less decline of body weight than cisplatin, as shown in **Fig. 11**. Furthermore, the toxicity was further investigated by histological images in major organs (liver, heart, lung, kidney and spleen) through H&E staining. It was noted that there was no obvious damage to major organs after treatments with complex **19** in three weeks (**Fig.12**). In contrast, serious damage to the major organ was observed in mice treated with cisplatin, consistent with the loss of body weight (**Fig. 11** C). In short, complex **19** showed high antitumor activity and low toxicity both *in vitro* and *in vivo*, and deserved further study.

3. Conclusions

In summary, four Pt(IV) prodrugs derived from cisplatin and oxaliplatin with two CA-4 analogues as an inhibitor of tubulin were designed and synthesized. *In vitro* assays revealed that all the resulting Pt(IV) complexes not only exhibited higher anticancer activities than their mother Pt(II) counterparts against tested human cancer cells, but also indicated less toxic than their corresponding Pt(II) complexes against two normal human cells. Among them, complex **19**, the Pt(IV) derivative from cisplatin with one CA-4 analogue ligand in the axial position, possessed better antitumor activities against three cancer cell lines (HCT-116, HepG-2 and MGC-803) than cisplatin with a 11.8-21.8 fold increase in activity. Interestingly, the activity of complex **19** was also sensitive to cisplatin resistant cancer cells (SK-OV-3/CDDP, IC_{50}=0.35±0.12) when compared with cisplatin sensitive cells (SK-OV-3, IC_{50}=0.28±0.16 μmol/L). Importantly, complex **19** significantly caused cell cycle arrest at G2/M phase and obviously disrupted the microtubule organization, and altered the expression of cell cycle-related proteins. Moreover, complex **19** effectively induced cell apoptosis and decreased MMP. Molecular mechanism studies indicated that complex **19** caused apoptotic cell death of human cancer cells SK-OV-3 through the mitochondrial mediated pathway by producing reactive oxygen species (ROS), down-regulating Bcl-2, up-regulating Bax, and further proteolytically activating downstream caspase-9 and -3. More importantly, the antitumor efficacy of complex **19** was verified in ovarian cancer xenograft mouse models with almost no toxicity. Complex **19** significantly suppressed the tumor volume and reduced tumor weight by 53.1% and 60.5% at doses of 5 mg/kg and 13 mg/kg/7 days (iv) in an SK-OV-3 ovarin cancer xenograft nude mice model, which was greater than that of the positive

control, CA-4 (51.6%). Our study indicated that complex **19** displayed significant antitumor efficacy both *in vitro* and *in vivo*, which has the potential to be further developed as a promising antitumor agent. Consequently, Pt(IV) anticancer prodrugs containing a tubulin inhibitor moiety can effectively inhibit tubulin polymerization that may be a promising approach for multiple targeted cancer therapy.

4. Experimental section

All chemicals and solvents were analytical reagent grade and commercially available, and used without further purification unless noted specifically. Column chromatography was performed using silica gel (200–300 mesh). Mass spectra were measured on an Agilent 6224 TOF LC/MS instrument. Elemental analyses of C, H, and N used a Vario MICRO CHNOS elemental analyzer (Elementary). ^{1}H NMR and ^{13}C NMR spectra were recorded in $CDCl_3$ or d^6-DMSO with a Bruker 300, 400 or 600 MHz NMR spectrometer.

*4.1 The released ability of compound **19** under reduction with ascorbic acid*

The ability of compound **19** to release the active platinum species and compound 13 under reducing condition was studied. Reduction of compound **19** (0.1 mmol/L) was carried out using ascorbic acid (0.5 0.1 mmol/L) in a solution of acetonitrile/water (65:35, V/V) and the resulting product was detected by HPLC and peak detection at 254 nm under UV. The incubation was generated by adding the test compounds to a solvent containing 65% acetonitrile and 35% water, which was carried out for 0 h, 2 h, 4 h, 6 h, 8 h, 10 h and 12 h at 37 □, respectively. Pure compound **19** was served as control to match the compound **18** peak in the HPLC chromatogram. Reversed-phase HPLC was performed with a 250 4.5 mm ODS column. Mobile phase comprised of acetonitrile/water (V/V ¼ 65:35, 0.1% TFA), and flow rate was 1.0 mL/min. The samples were taken for HPLC.

4.2. Cell culture and maintenance.

All human cancer cells and two human normal cells were purchased from China Life Science Collage (Shanghai, PRC). Culture medium Dulbecco's modified Eagle medium (DMEM), fetal bovine serum (FBS), phosphate buffered saline (PBS, pH=7.2), and Antibiotice-Antimycotic came from Jiangsu KeyGen Biotech Company (China). Cell lines were grown in the supplemented with 10% FBS, 100 units/ml of penicillin and 100 g/ml of streptomycin in a humidified atmosphere of 5% CO_2 at 37 ^{o}C.

4.3. Cytotoxicity assay.

The target complexes were dissolved in DMF and evaluated in three human cancer cells (HCT-116, HepG-2 and MGC-803) and two human normal cells (NCM460 and HL7702) as well as cisplatin-sensitive and resistant cells (SK-OV-3 and SK-OV-3/CDDP), respectively. About 5.0×10^4 cells/mL cells, which were in the logarithmic phase, were seeded in each well of 96-well plates and incubated for 12 h at 37 °C in 5% CO_2. Complexes at five different concentrations (1.25, 2.5, 5, 10 and 20 μmol/L) were added to the test well and then the cells were incubated at 37 °C in a 5% CO_2 atmosphere for 72 h. An enzyme labeling instrument was used to read absorbance with 570/630 nm double wavelength measurement. Cytotoxicity was detected on the percentage of cell survival compared with the negative control. The final IC_{50} values were calculated by the Bliss method (n = 5). All of the tests were repeated in triplicate.

4.4. Apoptosis analysis.

Apoptosis was investigated by flow cytometric analysis of annexin V/PI staining. SK-OV-3 cells were seeded in each well of six-well plates at the density of 5.0×10^4 cells/mL of the DMEM medium with 10% FBS to the final volume of 2 mL. The plates were incubated for overnight and treated with complex **19** and cisplatin at the indicated concentrations for 24 h. Briefly, cells were harvested and washed with twice ice-cold PBS, and then suspended cells in the annexin-binding buffer at a concentration of 2×10^5 cells /ml. Cells were then incubated with 5 μL of annexin V-FITC and 5 μL of PI in the dark at 4 °C for 20 minutes. The cells were examined by system software (Cell Quest; BD Biosciences).

4.5. Hoechst 33258 staining.

SK-OV-3 cells (5.0×10^4 cells) were seeded in six-well tissue culture plates and exposed to different concentrations (5 and 10 μmol/L) of complex **19** for 24 h. Untreated cells was served as negative control and cells treated with cisplatin (10 μmol/L) was acted as positive control. The cells were fixed in 4% paraformaldehyde for 10 min, and the cells were then washed twice with cold PBS and incubated with 0.5 mL of Hoechst 33258 at dark for 10 min. After 10 min incubation, the cells were washed twice with cold PBS and the results were analysis by a Nikon ECLIPSETE2000-S fluorescence microscope using 350 nm excitation and 460 nm emissions.

4.6. Cell uptake.

SK-OV-3 cells were seeded in each well of 96-well plates. After the cells reached about 80%

confluence, 5 and 10 μmol/L of complex **19** and cisplatin were added and the plates were also incubated for 24 h at 37 °C in 5% CO_2, respectively. After completion of 24 h incubation, cells were collected and washed three times with ice-cold PBS, then centrifuged at 1000×g for 10 min and resuspended in 2 mL PBS. A volume of 100 μL was taken out to examine the cell density. The remaining cells were digested by HNO_3 (200 μL, 65%) at 65 ^{o}C for 12 h, and then the Pt level in cells were examined by ICP-MS.

4.7. TUNEL assay.

TUNEL assay was performed as described previously. [35] The TUNEL method was performed to label 3-end of fragmented DNA of the apoptotic SK-OV-3 cells. SK-OV-3 cells (5.0×10^4 cells) were seeded in six-well tissue culture plates and exposed to different concentrations (5 and 10 μmol/L) of complex **19** for 24 h. Untreated cells was served as negative control and cells treated with cisplatin (10 μmol/L) was acted as positive control. After 24 h, the cells were washed two times with ice-PBS and then fixed with 4% paraformaldehyde. The staining was carried out according to the manufacturer's protocol. The FITC-labeled TUNEL-positive cells were imaged under a fluorescent microscopy by using 488 nm excitation and 530 nm emission.

4.8. Cell cycle analysis.

SK-OV-3 cells were seeded in 6-well plates and treated with complex **19** and cisplatin at the indicated concentrations and maintained with of the proper culture medium in 5% CO_2 at 37 °C for 24 h. After completion of incubation, cells were harvested and washed two times with ice-cold PBS, fixed with ice-cold 70% ethanol at -20 °C for overnight. The cells were treated with 100 μg /mL RNase A for 30 minutes at 37 °C after washed with two times ice-cold PBS, and finally stained with 1 mg/ml propidium iodide (PI) in the dark at 4 °C for 30 minutes. Analysis was performed with the system software (Cell Quest; BD Biosciences).

4.9. Immunofluorescence assay.

SK-OV-3 cells (5.0×10^4 cells) were seeded in 6-well plates and treated with complex **19** and CA-4 at the indicated concentrations and maintained with the proper culture medium in 5% CO_2 at 37 °C for 24 h. After being washed three times with ice-PBS and fixed in 4% paraformaldehyde at 37 °C for 20 minutes, then the cells were permeabilized with 0.5% Triton X-100 for 15 min and blocked for 30 minutes in 10% goat serum. The cells were incubated overnight with primary antibody (α-tubulin) at 4 °C. In the next day the cells were washed three times with ice-PBS, and

cells were incubated with corresponding fluorescence-conjugated secondary antibody for 1 h. After the nuclei of cells were stained with DAPI in the dark at room temperature for 30 minutes. Cells were visualized using a fluorescence microscopy.

4.10. Mitochondrial membrane potential (MMP) assay.

SK-OV-3 cells were seeded in six-well plates at the density of 5.0×10^4 cells/mL of the DMEM medium with 10% FBS to the final volume of 2 mL. The cells were treated with or without tested compounds at the indicated concentrations for 24 h. After incubation for 24 h, the cells were then stained with 2 μmol/L JC-1 at room temperature for 30 min and washed three times with ice-PBS, and the cell nuclei were stained with Hoechst 33258 for 20 minutes at room temperature in the dark. The emission fluorescence for JC-1 was monitored at 530 and 590 nm, under the excitation wavelength at 488 nm, respectively.

4.11. ROS assay

SK-OV-3 cells were seeded in six-well plates and treated with complex **19** and cisplatin at the indicated concentrations and maintained with of the proper culture medium in 5% CO_2 at 37 °C for 24 h. After completion of incubation, cells were harvested at 2000 rpm and washed three times with ice-cold PBS, and then resuspend cells in 10 mM DCFH-DA (Molecular Probe, Beyotime, Haimen, China) dissolved in cell free medium at 37 °C for 30 min in dark, and then washed twice with PBS. Cellular fluorescence was detected by flow cytometry at an excitation of 485 nm and an emission of 538 nm, respectively.

4.12. Western blot analysis

Western blot analysis was performed as described previously. [36] SK-OV-3 cells were treated with complex **19** and cisplatin at the indicated concentrations for 24 h, respectively. After incubation for 24 h, cells were collected, centrifuged, and washed three times with ice-cold PBS. The pellet was then resuspended in lysis buffer. After the cells were lysed on ice for 30 min, lysates were centrifuged at 20000g at 4 °C for 5 min. The protein concentration in the supernatant was examined using the BCA protein assay reagents (Imgenex, USA). Equal amounts of protein per line were was separated on 12% SDS polyacrylamide gel electrophoresis and transferred to PVDF Hybond-P membrane (GE Healthcare). Membranes were incubated with 5% skim milk in Tris-buffered saline with Tween 20 (TBST) buffer for 1 h and then the membranes being gently rotated overnight at 4 °C. Membranes were then incubated with primary antibodies against Bcl-2,

Bax, caspase-9, caspase-3 or GAPDH for overnight at 4 °C. Membranes were next incubated with peroxidase labeled secondary anti-bodies for 2 h, and then all membranes were washed with TBST three times for 15 minutes and the protein blots were detected with chemiluminescence reagent (Thermo Fischer Scientifics Ltd.). The X-ray films were developed with developer and fixed with fixer solution.

4.13. Antitumor Activity in vivo.

The in vivo cytotoxic activity of complex **19** was evaluated using human ovarian cells (SK-OV-3) in BALB/c nude mice. Five-week-old female BALB/c nude mice were purchased from Shanghai Ling Chang biotechnology company (China); tumors were induced by a subcutaneous injection in their dorsal region of 1.0×10^7 cells in 100 μL of sterile PBS. Animals were randomly divided into six groups, and started on the second day. When the tumors reached a volume of 100-150 mm^3 in all mice on day 18, the first group was injected with an equivalent volume of 5% dextrose via a tail vein as the vehicle control mice. No. 2 and No. 3 groups were treated with complex **19** at doses of 5 mg/kg and 13 mg/kg once a week for three weeks, respectively. No. 4 group was treated with cislatin at the dose of 5 mg/kg. No. 5 group was treated with CA-4 at the dose of 5 mg/kg. No. 6 group was treated with cisplatin/CA-4 mixture at the dose of 5 mg/kg + 5 mg/kg once a week for three weeks. All tested compounds were dissolved in vehicle. Tumor volume and body weight were recorded every other day after drug treatment. All mice were sacrificed after three weeks of treatment and the tumor volumes were measured with electronic digital calipers and determined by measuring length (A) and width (B) to calculate volume ($V = AB_2/2$).

4.14. H&E staining.

Tumor samples were shown in routine histopathological examination using Hematoxylin and Eosin (H&E) staining. Mouse organs (liver, heart, lung, kidney and spleen) were collected in 4% paraformaldehyde for proper fixation and then embedded in paraffin using tissue embedding machine. Sections were cut and stained with H&E staining. Briefly, sections were prepared orderly by dewaxing, stainingm and dehydration. After staining in Harris hematoxylin solution, sections were stained in eosin-phloxine solution for 1 min and then dehydrated and mounted with neutral resin. The tissue morphology was then observed under fluorescence microscopy using an Eclipse E800 Nikon (Nikon, Tokyo, Japan).

4.15. Statistical analysis.

All statistical analysis was performed with SPSS Version 10. Data was analyzed by one-way ANOVA. Mean separations were performed using the least significant difference method. Each experiment was replicated thrice, and all experiments yielded similar results. Measurements from all the replicates were combined, and treatment effects were analyzed.

Acknowledgments

We are grateful to the National Natural Science Foundation of China (Grant Nos. 21571033, 21431001 and 81760626) and the New Drug Creation Project of the National Science and Technology Major Foundation of China (Grant No. 2015ZX09101032) for financial aids to this work. The authors would also like to thank the Fundamental Research Funds for the Central Universities (Project 2242016K30020) for supplying basic facilities to our key laboratory. We also want to express our gratitude to the Priority Academic Program Development of Jiangsu Higher Education Institutions for the construction of fundamental facilities (Project 1107047002). The research was also supported by the Scientific Research Foundation of Graduated School of Southeast University (YBJJ1677).

Appendix A. Supplementary data

General procedure for the preparation of complexes **12-13** and **19-20** and figures.

References

[1] N. J. Wheate, S. Walker, G. E.Craig, R. Oun, The status of platinum anticancer drugs in the clinic and in clinical trials. *Dalton Trans*. 39 (**2010**) 8113–8127.

[2] E. Cvitkovic, M. Bekradda, Oxaliplatin: a new therapeutic option in colorectal cancer. *Semin. Oncol.* 26 (**1999**) 647–662.

[3] D. Wang, S. J. Lippard, Cellular processing of platinum anticancer drugs. *Nat. Rev. Drug Discovery*. 4 (**2005**) 307–320.

[4] N. Graf, S. J. Lippard, Redox activation of metal-based pro-drugs as a strategy for drug delivery. *Adv. Drug Delivery Rev.* 64 (**2012**) 993–1004.

[5] Z. H. Siddik, Cisplatin: mode of cytotoxic action and molecular basis of resistance. *Oncogene*. 22 (**2003**) 7265–7279.

[6] N. J. Wheate, S. Walker, G. E. Craig, R. Oun, The status of platinum anticancer drugs in the clinic and in clinical trials. *Dalton Trans.* 39 (**2010**) 8113–8127.

[7] R. P. Miller, R. K. Tadagavadi, G. Ramesh, W. B. Reeves, Mechanisms of cisplatin nephrotoxicity. *Toxins*. 2 (**2010**) 2490–2518.

[8] F. F. Liu, S. H. Gou, F. H. Chen, L. Fang, J. Zhao, Study on antitumor platinum(II) complexes of chiral diamines with dicyclic species as steric hindrance. *J. Med. Chem.* 58 (**2015**) 6368–6377.

[9] K. B. Huang, Z. F. Chen, Y. C. Liu, Z. Q. Li, J. H. Wei, M. Wang, G. H. Zhang, H. Liang, Platinum(II) complexes with mono-aminophosphonate ester targeting group that induce apoptosis through G1 cell-cycle arrest: Synthesis, crystal structure and antitumor activity. *Eur. J. Med. Chem*. 63 (**2013**) 76–84.

[10] K. B. Huang, Z. F. Chen, Y. C. Liu, Z. Q. Li, J. H. Wei, M. Wang, X. L. Xie, H. Liang, Platinum(II) complexes containing aminophosphonate esters: Synthesis, characterization, cytotoxicity and action mechanism. *Eur. J. Med. Chem*. 64 (**2013**) 554–561.

[11] A. Horwich, J. Shipley, R. Huddart, Testicular germ-cell cancer. *Lancet.* 367 (**2006**) 754–765.

[12] L. Kelland, The Resurgence of platinum-based cancer chemotherapy. *Nature Rev. Cancer.* 7 (**2007**) 573−584.

[13] X. P. Han, J. Sun, Y. J. Wang, Z. G. He, Recent advances in platinum (IV) complex-based delivery systems to improve platinum (II) anticancer therapy. *Med. Res. Rev*. 6 (**2015**) 1268−1299.

[14] X. Y. Wang, X. H. Wang, Z. J. Guo, Functionalization of platinum complexes for biomedical applications. *Acc. Chem. Res.* 48 (**2015**) 2622−2631.

[15] L. L. Ma, R. Ma, Y. P. Wang, X. Y. Zhu, J. L. Zhang, H. C. Chan, X. F. Chen, W. J. Zhang, S. K. Chiuc, G. Y. Zhu, Chalcoplatin, a dual-targeting and p53 activator containing anticancer platinum(IV) prodrug with unique mode of action. *Chem. Commun*. 51 (**2015**) 6301−6304.

[16] J. Ma, Q. P. Wang, Z. L. Huang, X. D. Yang, Q. D. Nie, W. P. Hao, P. G. Wang, X. Wang, Glycosylated platinum(IV) complexes as substrates for glucose transporters (GLUTs) and organic cation transporters (OCTs) exhibited cancer targeting and human serum albumin binding properties for drug delivery. *J. Med. Chem*. 60 (**2017**) 5736−5748.

[17] R. Raveendran, J. P. Braude, E. Wexselblatt, V. Novohradsky, O. Stuchlikova, V. Brabec, V. Gandin, D. Gibson, Pt(IV) Derivatives of cisplatin and oxaliplatin with phenylbutyrate axial ligands are potent cytotoxic agents that act by several mechanisms of action. *Chem. Sci.* 7

(**2016**) 2381–2391.

[19] X. C. Huang, R. Z. Huang, S. H. Gou, Z. M. Wang, Z. X. Liao, H. S. Wang, Combretastatin A-4 analogue: A dual-targeting and tubulin inhibitor containing antitumor Pt(IV) moiety with a unique mode of action. *Bioconjugate Chem*. 27 (**2016**) 2132−2148.

[20] R. K. Pathak, S.Marrache, J. H.Choi, T. B.Berding, S.Dhar, The Pro-drug platin-A: simultaneous release of cisplatin and aspirin. *Angew. Chem. Int. Ed.* 53 (**2014**) 1963–1967.

[21] X. D. Qin, L. Fang, F. H. Chen, S. H. Gou, Conjugation of platinum(IV) complexes with chlorambucil to overcome cisplatin resistance via a “joint action” mode toward DNA. *Eur. J. Med. Chem.* 137 (**2017**) 167–175.

[22] F. H. Chen, X. C. Huang, M. Wu, S. H. Gou, W. W. Hu, A CK2-targeted Pt(IV) prodrug to disrupt DNA damage response. *Cancer Lett*. 385 (**2017**) 168−178.

[23] G. R. Pettit, S. B. Singh, E. Hamel, C. M. Lin, D. S. Alberts, D. Garcia-Kendall, Isolation and structure of the strong cell growth and tubulin inhibitor combretastatin A-4. *Experientia*. 45 (**1989**) 209–211.

[24] H. Chen, Y. M. Li, C. Q. Sheng, Z. L. Lv, G. Q. Dong, T. T. Wang, J. Liu, M. F. Zhang, L. Z. Li, T. Zhang, D. P. Geng, C. J. Niu, K. Li, Design and synthesis of cyclopropylamide analogues of combretastatin-A 4 as novel microtubule-stabilizing agents. *J. Med. Chem.* 56 (**2013**) 685–699.

[25] G. Attard, A. Greystoke, S. Kaye, J. Bono De, Update on tubulin-binding agents. *Pathol. Biol. (Paris)*. 54 (**2006**) 72–84.

[26] R. P. George, M. R. Rhodes, D. L. Herald, E. Hamel, J. M. Schmidt, R. K. Pettit, Antineoplastic agents. 445. Synthesis and evaluation of structural modifications of (*Z*)- and (*E*)-combretastatin A-4. *J. Med. Chem.* 48 (**2005**) 4087–4099.

[27] P. Suman, T. R. Murthy, K. Rajkumar, D. Srikanth, C. Dayakar, C. Kishor, A. Addlagatta, S. V. Kalivendi, B. C. Raju, Synthesis and structureeactivity relationships of pyridinyl-1H-1,2,3-triazolyldihydroisoxazoles as potent inhibitors of tubulin polymerization. *Eur. J. Med. Chem.* 90 (**2015**) 603–619.

[28] A. Kamal, A. Mallareddy, M. J. Ramaiah, S. Pushpavalli, P. Suresh, C. Kishor, J. Murty, N. S. Rao, S. Ghosh, A. Addlagatta, M. Pal-Bhadra, Synthesis and biological evaluation of combretastatin-amidobenzothiazole conjugates as potential anticancer agents. *Eur. J. Med.*

Chem. 56 (**2012**) 166–178.

[29] V. Chaudhary, J. B. Venghateri, H. P. Dhaked, A. S. Bhoyar, S. K. Guchhait, D. Panda, Novel combretastatin-2-aminoimidazole analogues as potent tubulin assembly Inhibitors: exploration of unique pharmacophoric impact of bridging skeleton and aryl moiety. *J. Med. Chem*. 59 (**2016**) 3439–3451.

[30] V. Peyrot, C. Briand, R. Momburg, J. C. Sari, *In vitro* Mechanism Study of Microtubule Assembly Inhibition by cisdichlorodiammine-platinum (II). *Biochem. Pharmacol*. 35 (**1986**) 371–375.

[31] R. Schobert, B. Biersack, A. Dietrich, S. Knauer, M. Zoldakova, A. Fruehauf, T. Mueller, Pt (II) Complexes of a Combretastatin A-4 Analogous Chalcone: Effects of Conjugation on Cytotoxicity, Tumor Specificity, and Long-Term Tumor Growth Suppression. *J. Med. Chem.* 52 (**2009**) 241–246.

[32] M. Ravera, E. Gabano, G. Pelosi, F. Fregonese, S. Tinello, D. Osella, A New Entry to Asymmetric Platinum(IV) Complexes via Oxidative Chlorination. *Inorg. Chem.* 53 (**2014**) 9326−9335.

[33] Y. Gou, J. Wang, S. F. Chen, Z. Zhang, Y. Zhang, W. Zhang, F. Yang, a-N-heterocyclic thiosemicarbazone Fe(III) complex: Characterization of its antitumor activity and identification of anticancer mechanism. *Eur. J. Med. Chem.* 123 (**2016**) 354−364.

[34] E. R. Jamieson, S. J. Lippard, Structure, recognition, and processing of cisplatin-DNA adducts. *Chem. Rev*. 99 (1999) 2467−2498.

[35] X. C. Huang, L. Jin, M. Wang, D. Liang, Z. F. Chen, Y. Zhang, Y. M. Pan, H. S. Wang, Design, synthesis and in vitro evaluation of novel dehydroabietic acid derivatives containing a dipeptide moiety as potential anticancer agents. *Eur. J. Med. Chem.* 89 (**2015**) 370−385.

[36] S. H. Huang, L. W. Wu, A. C. Huang, C. C. Yu, J. C. Lien, Y. P. Huang, J. S. Yang, J. H. Yang, Y. P. Hsiao, W. G. Wood, C. S. Yu, J. G. Chung, Benzyl isothiocyanate (BITC) induces G2/M phase arrest and apoptosis in human melanoma A375.S2 cells through reactive oxygen species (ROS) and both mitochondria-dependent and death receptor-mediated multiple signaling pathways. *J. Agric. Food Chem*. 60 (**2012**) 665−675.

[37] M. Kamachi, T. M. Le, S. J. Kim, M. E. Geiger, P. Anderson, P. J. Utz, Human autoimmune sera as molecular probes for the identification of an autoantigen kinase signaling pathway. *J.*

Exp. Med. 196 (**2002**)1213−1225.

[38] J. Wang, J. Yi, Cancer cell killing via ROS: to increase or decrease, that is the question. *Cancer Biol. Ther.* 7 (**2008**) 1875−1884.

[39] Z. F. Chen, Q. P. Qin, J. L. Qin, Y. C. Liu, K. B. Huang, Y. L. Li, T. Meng, G. H. Zhang, Y. Peng, X. J. Luo, and H. Liang, Stabilization of G-Quadruplex DNA, inhibition of telomerase activity, and tumor cell apoptosis by organoplatinum(II) complexes with oxoisoaporphine. *J. Med. Chem*. 58 (**2015**) 2159−2179.

[40] M. C. Wei, W. X. Zong, E. H. Y. Cheng, T. Lindsten, V. Panoutsakopoulou, A. J.Ross, K. A. Roth, G. R. MacGregor, C. B. Thompson, S. J. Korsmeyer, ProapoptoticBax and Bak: a requisite gateway to mitochondrial dysfunction and death. *Science*. 292 (**2001**) 727−730.

[41] J. X. Qi, Y. Gou, Y. Zhang, K. Yang, S. F. Chen, L. Liu, X. Y. Wu, T. Wang, W. Zhang, F. Yang, Developing anticancer ferric prodrugs based on the N-donor residues of human serum albumin carrier IIA subdomain. *J. Med. Chem.* 59 (**2016**) 7497−7511.

Schemes

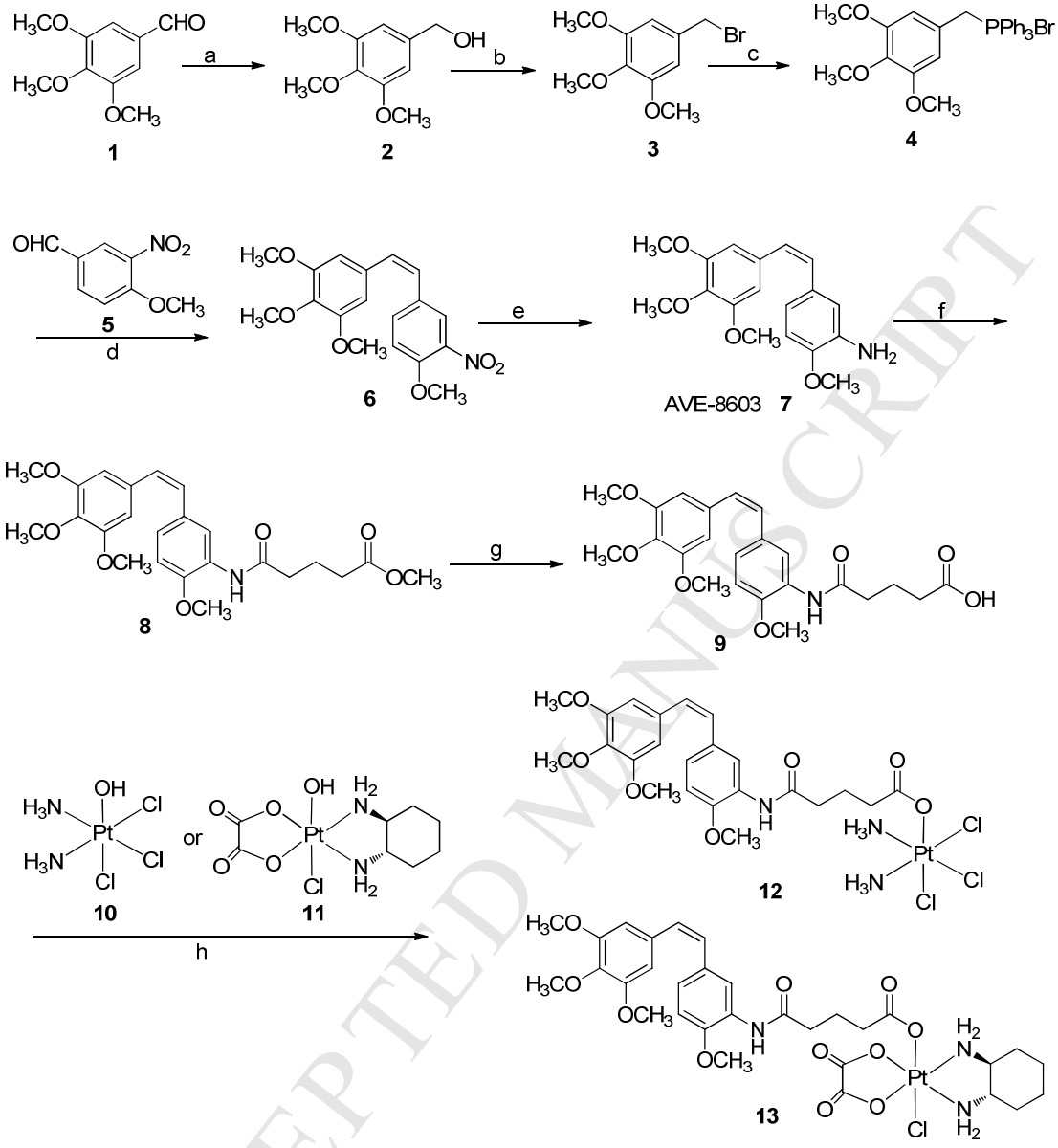

Scheme 1. Synthetic pathway to target complexes **12** and **13**. Reagents and conditions: (a) $NaBH_4$, CH_3OH, 0 ^oC; (b) PBr_3, CH_2Cl_2, 0 ^oC; (c) PPh_3, toluene, 110 ^oC; (d) NaH, CH_2Cl_2, room temperature; (e) Fe, NH_4Cl, EtOH, 85 ^oC; (f) EDCI, HOBT, Et_3N, DMF, 25 ^oC; (g) $LiOH \cdot H_2O$, THF/H_2O, 0 ^oC; (h) TBTU, Et_3N, DMF, 30 ^oC.

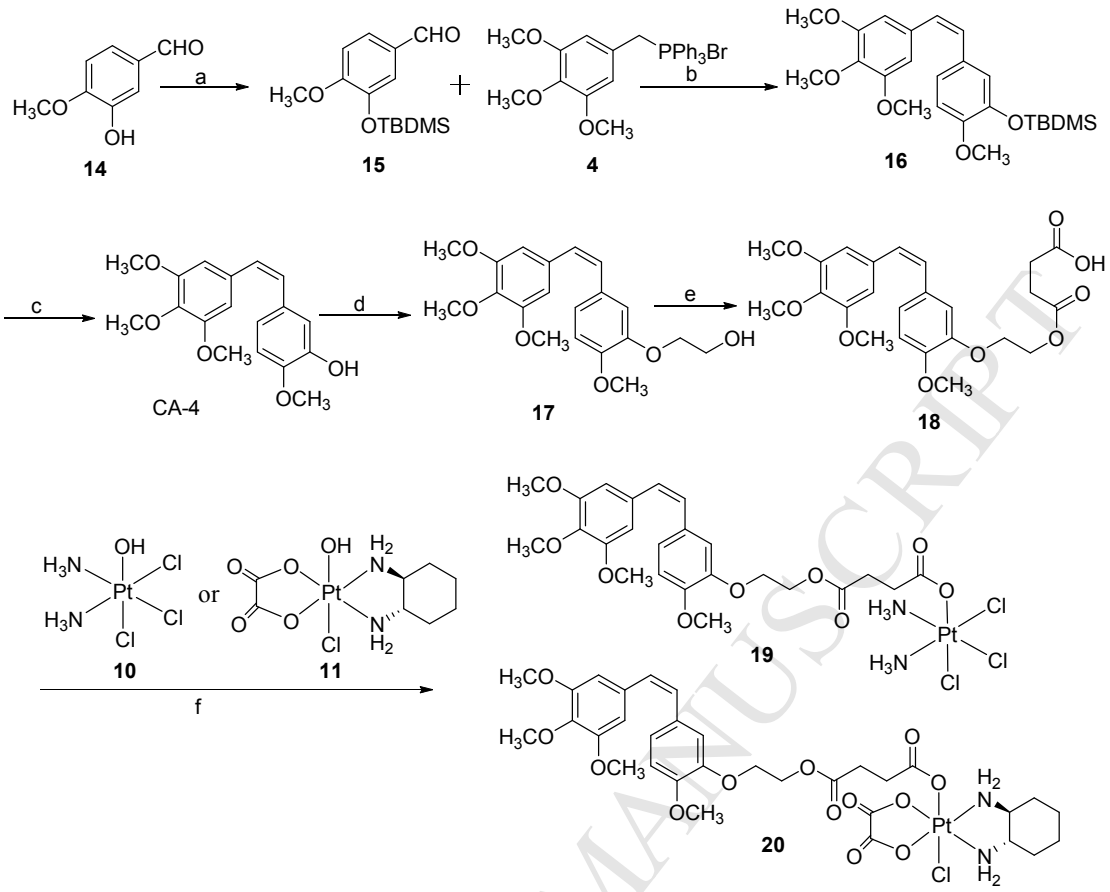

Scheme 2. Synthetic pathway to target complexes **19** and **20**. Reagents and conditions: (a) TBDMSCl, Et_3N, CH_2Cl_2, 0 ^oC; (b) NaH, CH_2Cl_2, 25 ^oC; (c) 1N HCl/CH_3OH, 50 ^oC; (d) 2-bromoethanol, K_2CO_3, DMF, 50 ^oC; (g) succinic anhydride, Et_3N, DMF, 50 ^oC; (h) TBTU, Et_3N, DMF, 30 ^oC.

Table 1. Cytotoxic effects of complexes **12-13** and **19-20** on human cancer and normal cell lines.

Compd.	IC_{50} (μmol/L) [a]						
	HCT-116	HepG-2	MGC-803	NCM460	HL-7702	SI [b]	SI [c]
9	1.82±0.51	3.24±0.89	1.95±0.60	14.29±1.89	11.21±1.76	7.9	3.5
12	0.62±0.27	0.97±0.38	0.74±0.52	22.74±2.58	20.24±1.52	36.7	20.9
13	0.75±0.34	1.21±0.27	0.53±0.21	24.46±2.17	25.46±2.04	32.6	21.0
18	1.05±0.41	2.25±0.36	1.61±0.44	15.16±1.55	12.07±1.13	14.4	5.4
19	0.41±0.18	0.71±0.23	0.39±0.15	17.86±2.07	19.35±1.87	43.6	49.6
20	0.52±0.41	1.06±0.55	0.73±0.59	20.24±2.16	23.28±2.61	38.9	21.9
7	0.13±0.05	0.14±0.06	0.24±0.15	7.37±1.36	6.27±1.08	56.7	44.8
17	0.82±0.47	1.84±0.69	0.65±0.58	10.61±1.77	9.95±1.71	12.9	5.4
CA-4	0.12±0.09	0.11±0.05	0.09±0.08	5.21±1.06	3.21±0.66	43.4	29.2
Cisplatin	8.95±1.08	8.36±0.89	7.81±1.03	15.82±1.93	10.85±0.91	1.8	1.3
Oxaliplatin	4.07±0.82	10.19±1.76	10.24±1.14	9.23±1.44	12.63±1.52	2.3	1.2

[a] *In vitro* cytotoxicity was determined by MTT assay upon incubation of the live cells with the compounds for 72 h. [b] Selectivity Index = IC_{50} (HCT-116) /IC_{50} (NCM460). [c] Selectivity Index = IC_{50}(HL-7702)/IC_{50}(HepG-2). Mean values based on three independent experiments.

Table 2. Biological activity of complexes **12-13** and **19-20** against cisplatin sensitive and resistant cancer cells (SK-OV-3 and SK-OV-3/CDDP).

Comp.	IC_{50} (μmol/L) [a]		
	SK-OV-3	SK-OV-3/CDDP	RF [b]
9	3.01±1.03	3.66±0.83	1.22
12	0.42±0.31	0.53±0.25	1.26
13	0.85±0.43	0.98±0.63	1.15
18	1.88±0.81	2.56±0.93	1.36
19	0.28±0.16	0.35±0.12	1.25
20	0.75±0.61	0.89±0.37	1.19
7	0.49±0.58	0.61±0.28	1.24

17	0.94±0.72	1.06±0.65	1.13
CA-4	0.17±0.19	0.21±0.11	1.24
Cisplatin	5.10±1.21	30.57±1.95	5.99
Oxaliplatin	9.37±1.39	23.05±2.13	2.46

[a] *In vitro* cytotoxicity was determined by MTT assay upon incubation of the live cells with the compounds for 72 h. [b] RF (resistant factor) is defined as IC_{50} in SK-OV-3CDDP/IC_{50} in SK-OV-3. Mean values based on three independent experiments, and the results of the representative experiments are shown.

Table 3. Cellular uptake of complex **19** in SK-OV-3 cells after 24 h of incubation.

	Pt content (ng/10^6 cells)
Comp.	SK-OV-3
19 (5 μmol/L)	335±31
19 (10 μmol/L)	709±70
Cisplatin (5 μmol/L)	198±20
Cisplatin (10 μmol/L)	323±31

The experiments were performed three times, and the results of the representative experiments are shown.

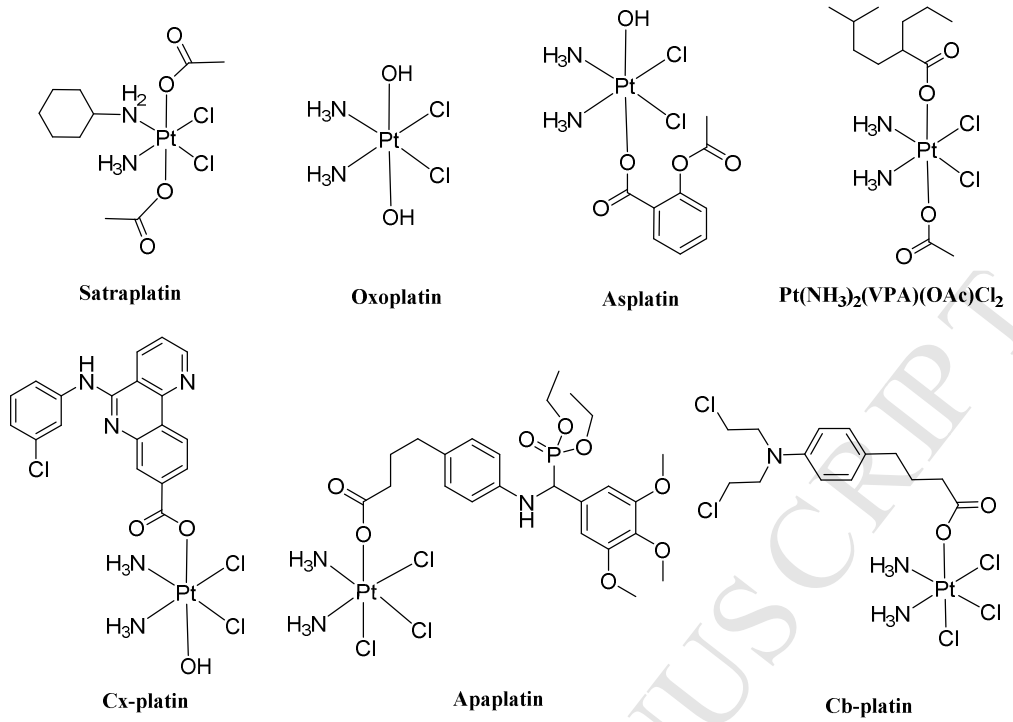

Fig. 1. Chemical structures of some Pt(IV) complexes as prodrugs.

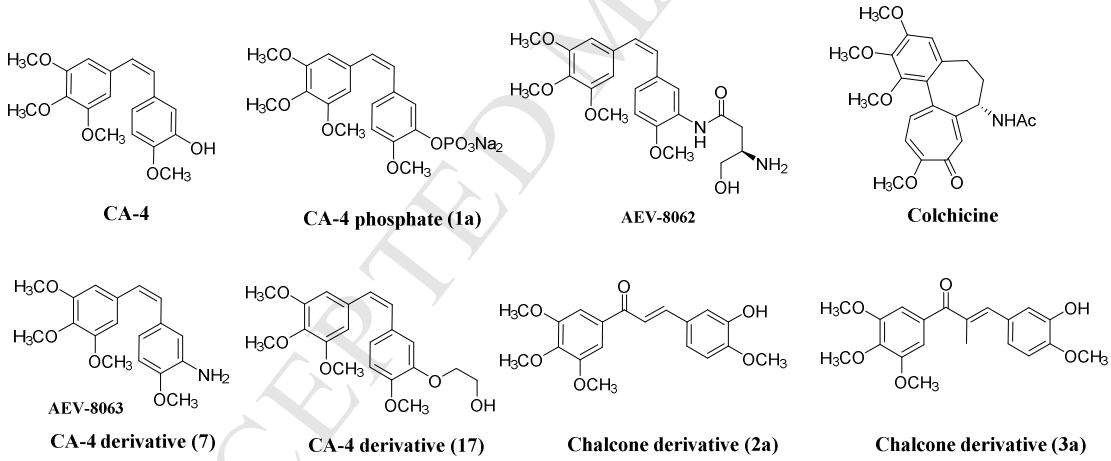

Fig. 2. Some tubulin interacting agents and lead structures.

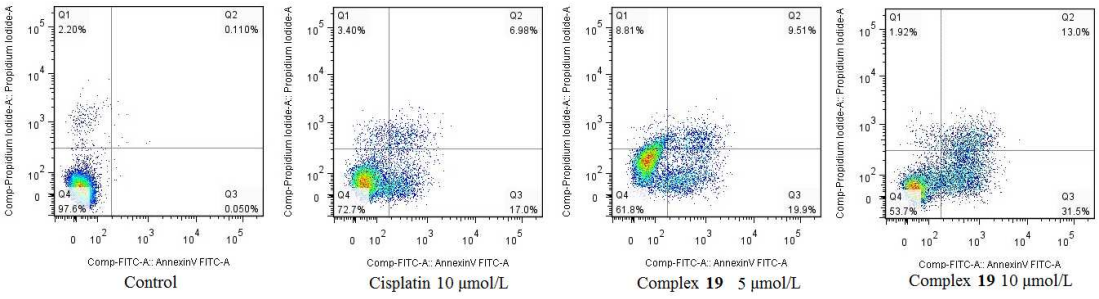

Fig. 3. Representative flow cytometric histograms of apoptotic SK-OV-3 cells after 24 h treatment

with complex **19** (5 and 10 μmol/L) and cisplatin (10 μmol/L) as positive control. The cells were harvested and labeled with annexin-V-FITC and PI, and analyzed by flow cytometry. Data are expressed as the mean ± SEM for three independent experiments.

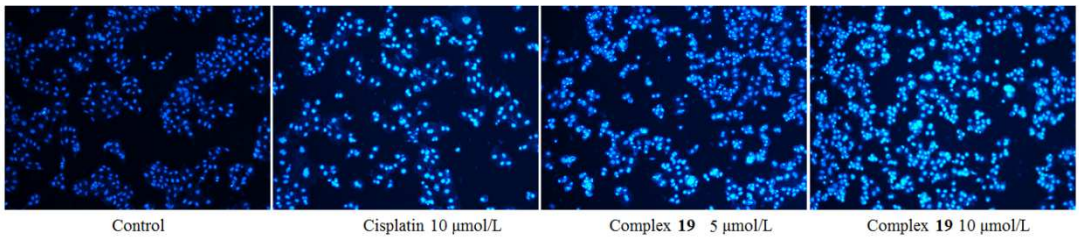

Fig. 4. Morphological changes in the nuclei (typical of apoptosis) of SK-OV-3 cells treated with complex **19** and cisplatin at the indicated concentrations for 24 h, respectively. Then, the cells were harvested, and stained by Hoechst 33258. The cells were analyzed by the Nikon Te2000 deconvolution microscope (magnification 200×). The experiments were performed three times, and the results of the representative experiments are shown.

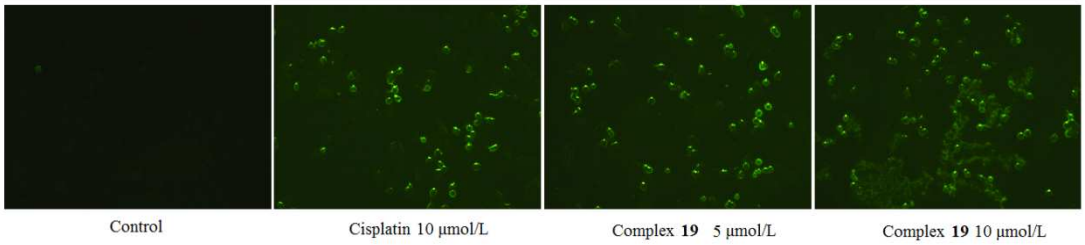

Fig. 5. TUNEL assay of complex **19** in SK-OV-3 cells. Cells treated with complex **19** and cisplatin at the indicated concentrations for 24 h, respectively. Selected fields illustrating condensed chromatin (white arrow heading) as occurrence of cell apoptosis were shown. Images were visualized by fluorescence microscope. The experiments were performed three times, and the results of the representative experiments are shown.

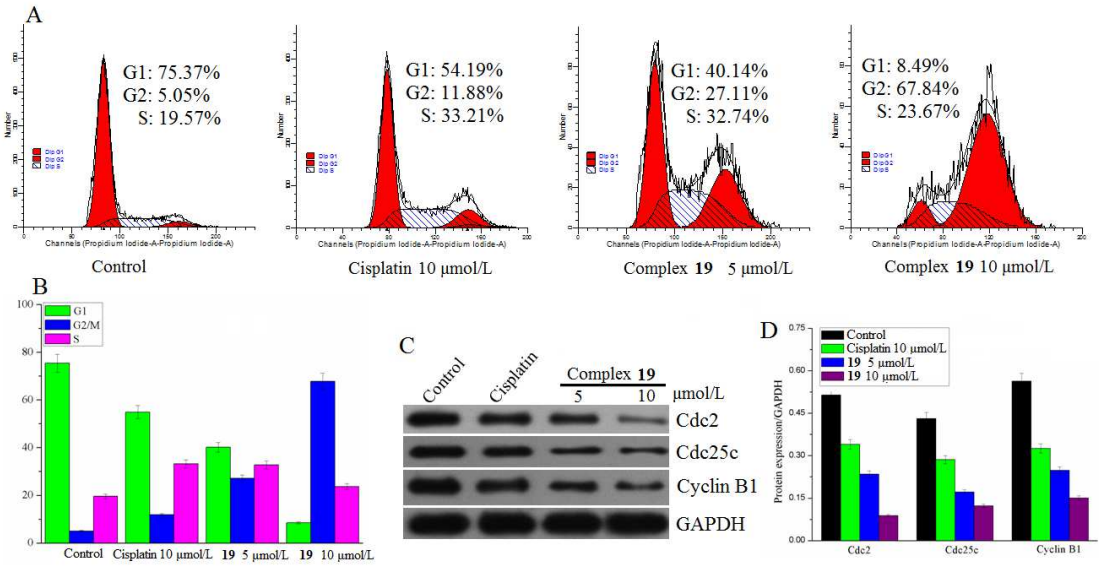

Fig. 6. (A) Cell cycle arrest effect of complex **19**. SK-OV-3 cells treated with complex **19** and cisplatin at the indicated concentrations for 24 h. Then, the cells were trypsinized, harvested and washed three times with ice-PBS for PI-stained DNA content detected by flow cytometry. (B) Quantitative analysis of the percentage of cells in each cell cycle phase. (C) The total proteins were harvested for the Western blot analysis to detect the expression of Cdc2, Cdc25c and cyclin B1. (D) Expression levels of (C) shown as percentages. The experiments were performed three times, and the results of the representative experiments are shown. $P<0.05$

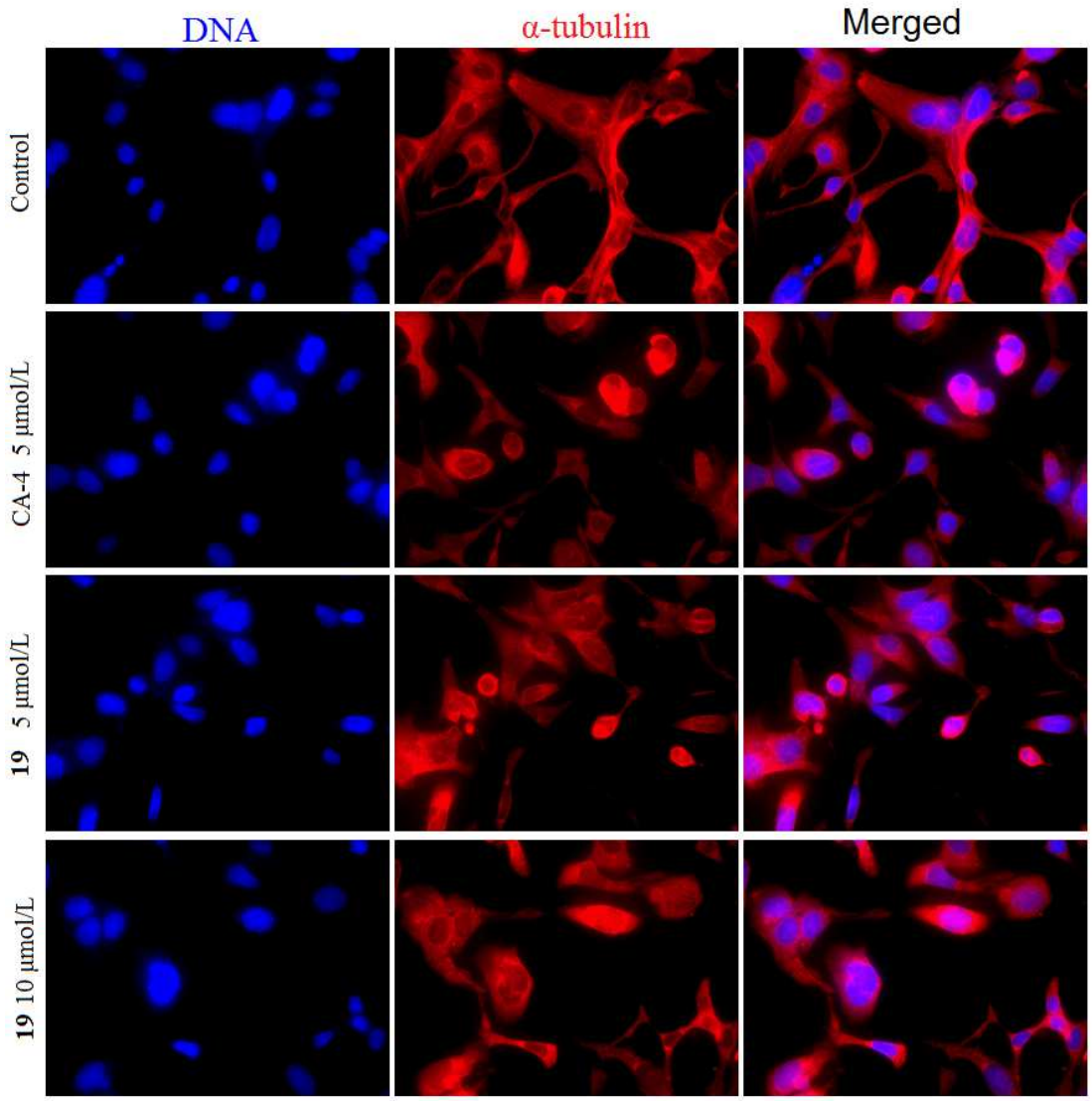

Fig. 7. Effect of complex **19** on the organization of cellular microtubule network. Untreated cells served as the negative control, and CA-4 as the positive drug. SK-OV-3 cells treated with complex **19** were fixed and stained with a-tubulin, and then counterstained with 4, 6-diamidino-2-phenylindole (DAPI). Microtubules and unassembled tubulin are shown in red. DNA, stained with DAPI, is shown in blue. The experiments were performed three times, and the results of the representative experiments are shown.

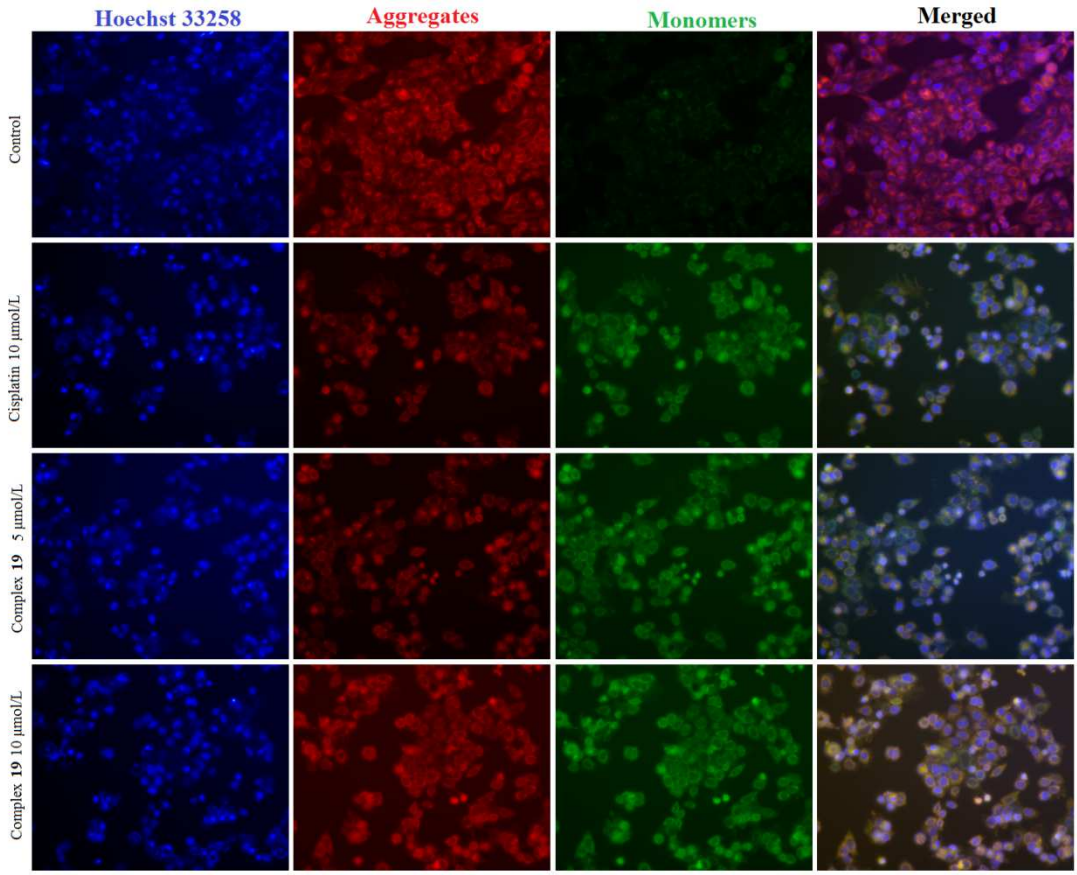

Fig. 8. Complex **19** decreased the MMP of SK-OV-3 cells. The cells were treated with **19** and cisplatin at the indicated concentrations for 24 h followed by incubation with the fluorescence probe JC-1 for 30 min. Then, the cells were analyzed by the Nikon Te2000 deconvolution microscope (magnification 200×). The experiments were performed three times, and the results of the representative experiments are shown.

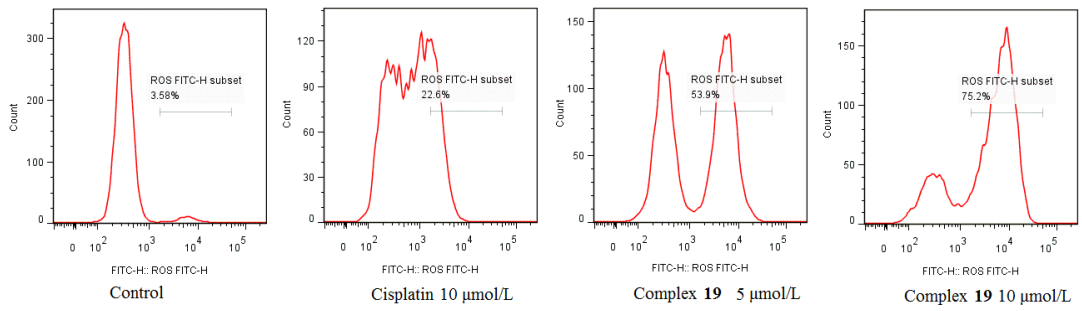

Fig. 9. Intracellular production of ROS by complex **19** and cisplatin following a 24 h incubation determined by flow cytometry. The experiments were performed three times, and the results of the representative experiments are shown.

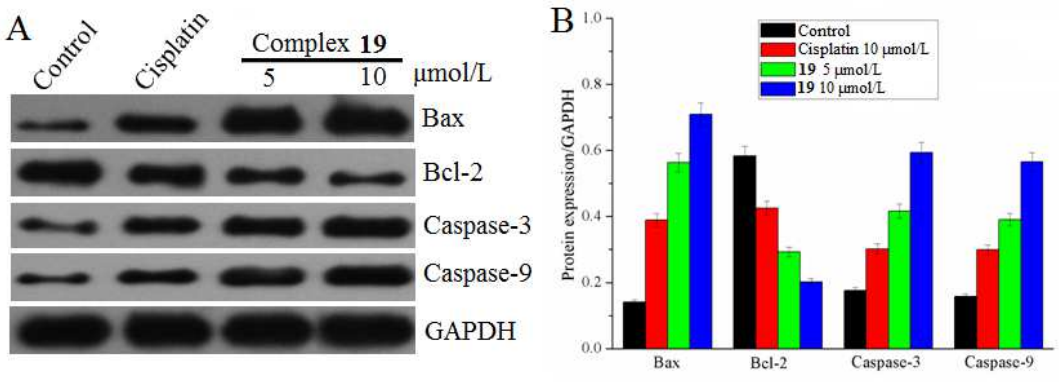

Fig. 10. (A) Immunoblotting analysis of proteins related to complex **19**-induced cell apoptosis. Whole-cell extracts were prepared and analyzed by Western blot analysis using antibodies against proteins indicated. The same blots were stripped and reprobed with GAPDH antibody to show equal protein loading. (B) Expression levels of (A) shown as percentages. The experiments were performed three times, and the results of the representative experiments are shown. * $P < 0.05$.

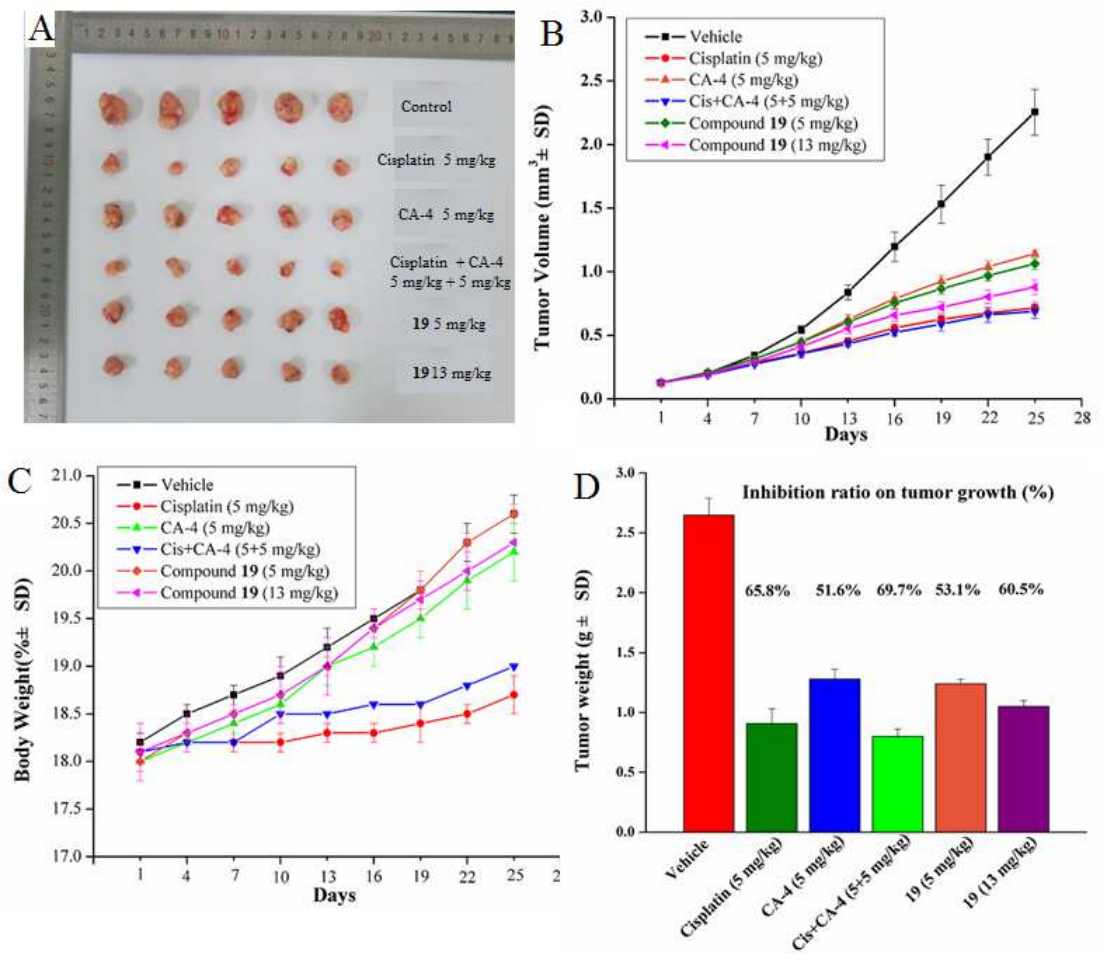

Fig. 11. *In vivo* antitumor activity of complex **19** in mice (BALB/c nude mice) bearing SK-OV-3

xenograft model. (A) After administered with complex **19** at the dose of 5 and 13 mg/kg iv once a week for 21 days, equal mass mixture of cisplatin and CA-4 at the dose of 5 mg/kg for iv once a week for 21 days, cisplatin and CA-4 at the dose of 5 mg/kg for iv once a week for 21 days, respectively, the mice were sacrificed and weighed the tumors. (B) The tumor volume of the mice in each group during the observation period. (C) The body weight of the mice from each group at the end of the observation period. (D) The weight of the excised tumors of each group. The data were presented as the mean ± SEM. IR=Inhibitory rate. *P < 0.05.

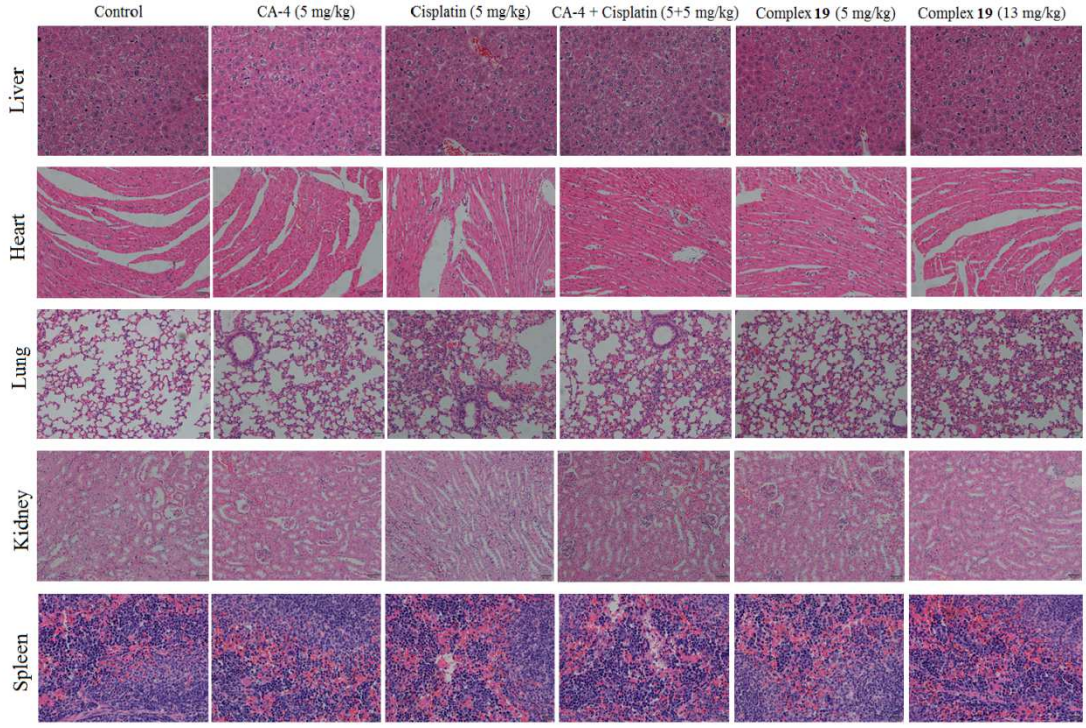

Fig. 12. After 21 days of treatment, the major organs (liver, heart, lung, kidney and spleen) were harvested from mice and then stained with H&E.

Highlights

- Novel Pt(IV) complexes containing CA-4 analogues can inhibit tubulin.
- The resulting Pt(IV) complexes exhibited certain ability to overcome cisplatin resistance.
- Complex **19** displayed higher cytotoxicity and lower toxicity than cisplatin.
- **19** effectively inhibited tumor growth in SK-OV-3 xenograft model *in vivo*.
- **19** might induce cell apoptosis through mitochondrion pathway.